Successive magnetic transitions of the kagome plane and field-driven chirality in single-crystal $BaMn_{2.49}Ru_{3.51}O_{11}$

L. Shlyk,[1,*] S. Parkin,[2] and L. E. De Long[1]
[1]*Department of Physics and Astronomy, University of Kentucky, Lexington, Kentucky 40506-0055, USA*
[2]*Department of Chemistry, University of Kentucky, Lexington, Kentucky 40506-0055, USA*
(Received 28 September 2009; revised manuscript received 22 December 2009; published 19 January 2010)

The magnetization of single-crystal $BaMn_{2.49}Ru_{3.51}O_{11}$ exhibits anomalies at temperatures $T_1=183$ K, $T_2=171$ K, and $T_3=128$ K, which signal complex magnetic order induced by competing ferro- and antiferromagnetic correlations, and magnetic frustration within the kagome (hexagonal **ab**) plane. The T_2 and T_3 anomalies and unconventional transverse magnetoresistance are observed only for magnetic field $\boldsymbol{H}$ applied in the kagome plane. We conclude a topological Hall effect is generated by nonzero scalar chirality of spins canted out of the kagome plane but is suppressed in a collinear structure induced by only modest in-plane fields.

DOI: 10.1103/PhysRevB.81.014413 PACS number(s): 75.50.Gg, 75.25.−j, 75.30.−m, 75.47.−m

Intriguing new phenomena, such as an anomalous Hall effect of topological origin (THE) (Refs. 1 and 2) and multiferroicity,[3] are found in canted or noncollinear magnetic structures induced by magnetic frustration. An example is a planar kagome lattice formed from corner-sharing triangles. Nearest-neighbor antiferromagnetic (AFM) interactions among Heisenberg spins on a kagome lattice generate large ground-state degeneracy but not long-range order. Weak perturbations, such as lattice disorder,[4] anisotropy,[5] and next-nearest-neighbor interactions,[6] can remove the degeneracy and induce long-range magnetic order. Many frustrated systems have complex crystal structures, and are available only in polycrystalline form; indeed, far less is known about the nature of the phase transitions of disordered kagome lattices of atomic spins $S>\frac{1}{2}$ than for $S=1/2$.[7,8]

The *R*-type ferrites $BaM_2Ru_4O_{11}$ (M=Fe, Mn, Co) crystallize in the hexagonal $P6_3/mmc$ structure[9,10] that has a kagome sublattice formed by edge-sharing octahedra $M(2)O_6$ that lie within the **ab** plane. The kagome planes are connected along [001] by face-sharing $M(1)O_6$ octahedra and trigonal bipyramids $M(3)O_5$ (Fig. 1). Single-crystal studies[11,12] of $(Ba,Sr)M_{2+x}Ru_{4-y}O_{11}$ ($x=y$ and M=Fe and Co) have revealed anisotropic electric and magnetic properties that can be widely varied with composition. The homogeneity range is generated by variable occupation of the octahedral $M(1)$ and $M(2)$ sites by 3*d* and 4*d* elements, while trigonal-pyramidal $M(3)$ sites are exclusively occupied by 3*d* elements.[11,12] In spite of potential magnetic frustration on the kagome sublattice, some compositions exhibit a unique coexistence of narrow-gap semiconductivity with ferrimagnetic order below unusually high critical temperatures $T_C \sim 490$ K, which makes *R*-type ferrites attractive for spintronic applications.[12]

A previous neutron powder refinement of a Mn-bearing ferrite of nominal composition $BaMn_2Ru_4O_{11}$ (Ref. 10) revealed the $M(3)$ sites underwent FM ordering along the **c** axis, whereas the $M(1)$ sites were nonmagnetic. Moreover, the spins $\boldsymbol{S_i}$ ($i=1, 2, 3$) that occupy each of the three vertices of triangular plaquettes in the kagome plane ordered in a two-dimensional, compensated motif characteristic of a frustrated lattice of magnetic ions with AFM nearest-neighbor interactions, as shown in Fig. 1. Neutron data taken at $T=100$ K were refined with an *in-plane*, "$q=0$" structure having uniform *vector chirality* $\boldsymbol{K}_V=[2/(3\sqrt{3})](\boldsymbol{S}_1\mathbf{x}\boldsymbol{S}_{2+}\boldsymbol{S}_2\mathbf{x}\boldsymbol{S}_3+\boldsymbol{S}_3\mathbf{x}\boldsymbol{S}_1)$ for the case of kagome triangles. Refinements for $T<100$ K indicated the $M(2)$ spins canted *out of the kagome plane*, inducing nonzero *scalar chirality* $K_S=\boldsymbol{S}_1\bullet(\boldsymbol{S}_2\times\boldsymbol{S}_3)$. A continuous increase of magnetic peak intensity culminated in an ordered moment $m=3.3\mu_B$ at $T=3.6$ K.

We have grown $BaMn_{2.49}Ru_{3.51}O_{11}$ single crystals that exhibit unique properties, including three closely spaced anomalies in the dc magnetization and a highly anisotropic transverse magnetoresistivity, which we report herein. We conclude competing magnetic interactions and frustration induce two or more magnetic phases whose spin chirality can be controlled using only modest fields $\mu_oH<1$ T applied within the kagome plane.

Single crystals of $BaMn_{2.49}Ru_{3.51}O_{11}$ with maximum basal-plane width 1.5 mm and thickness around 0.05 mm were grown from a $BaCl_2$ flux, as described elsewhere.[11] Single-crystal x-ray diffraction data for small, black, hexagonal platelets were collected at $T=90.0(2)$ K on a Nonius Kappa charge coupled device diffractometer using Mo-$K\alpha$ radiation ($\lambda=0.71073$ Å). Selected information on data col-

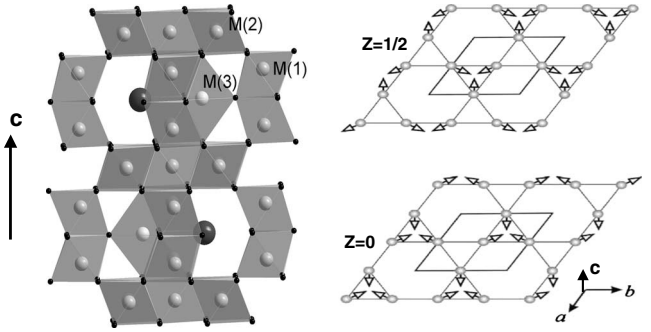

FIG. 1. Left panel: Crystal structure of $BaMn_{2.49}Ru_{3.51}O_{11}$. Right panel: **c**-axis projection of the kagome planes of $BaMn_{2.49}Ru_{3.51}O_{11}$ at the bottom ($Z=0$) and middle ($Z=1/2$) of the unit cell. The open arrows show the in-plane components of the moments on $M(2)$ sites. After Ref. 11.

TABLE I. Crystal data and structure refinement for $BaMn_{2.49}Ru_{3.51}O_{11}$.

Empirical formula	$BaMn_{2.49}Ru_{3.51}O_{11}$
Formula weight	1609.79
Temperature	90.0(2) K
Wavelength	0.71073 Å
Crystal system, space group	Hexagonal, $P63/mmc$
Unit cell dimensions	$a=5.8754(8)$ Å alpha=90°
	$b=5.8754(8)$ Å beta=90°
	$c=13.515(3)$ Å gamma=120°
Volume	404.04(11) $Å^3$
Z, Calculated density	1, 6.616 Mg/m^3
Absorption coefficient	15.000 mm^{-1}
Crystal size	$0.09\times0.08\times0.08$ mm
Theta range for data collection	3.01–27.45°
Limiting indices	$-7\leq h\leq 7$, $-7\leq k\leq 7$, $-17\leq 1\leq 17$
Reflections collected/unique	8346/212 [R(int)=0.0371]
Absorption correction	Semiempirical from equivalents
Refinement method	Full-matrix least squares on F^2
Goodness of fit on F^2	1.279
Final R indices [$I>2$ sigma(I)]	$R_1=0.0143$, $wR_2=0.0369$
R indices (all data)	$R_1=0.0148$, $wR_2=0.0371$
Extinction coefficient	0.0193(8)

lection and structure refinement are collected in Table I. Table II gives atomic coordinates and displacement parameters. Sample homogeneity and the absence of secondary phases were also ascertained by scanning electron microscope investigation. Several crystals were cleaved along, and perpendicular to the **c** axis, in order to expose interior surfaces for semiquantitative μ-probe analyses. Very consistent compositions were observed for all crystals and surfaces investigated, and the inferred atomic density ratio $n(\mathrm{Ru})/n(\mathrm{Mn})=1.4$ is in excellent agreement with the composition $BaMn_{2.5}Ru_{3.5}O_{11}$ inferred from the x-ray refinement. No additional elements were detected.

The dc magnetic moment m was measured over a temperature range $5\leq T\leq 300$ K in applied magnetic fields $0\leq \mu_o H\leq 5$ T using a Quantum Design magnetic property measurement system (MPMS)5 Magnetometer. Longitudinal and transverse magnetoresistivities, $\rho_{xx}(T)$ and $\rho_{xy}(H,\ T)$, respectively, were measured using the MPMS5 External Device Control Option and a dc four-probe method with currents $5\leq J\leq 20$ mA directed in the sample **ab** plane.

Our x-ray refinements and charge balance considerations suggest Mn^{3+} and mixed-valent Ru^{3+}/Ru^{5+} ions occupy the $M(2)O_6$ octahedra of the kagome plane. The magnetic susceptibility for $T>250$ K is isotropic and follows a Curie-Weiss law $\chi=C/(T-\Theta_{\mathrm{CW}})$ with $\Theta_{\mathrm{CW}}=+180$ K [signaling ferromagnetic (FM) interactions] and an effective moment $\mu_{eff}=3.7\mu_B$. This effective moment is in good agreement with the value $\mu_{eff}=3.4\mu_{\mathrm{B}}$ obtained using the refined composition and spin-only moments for Ru^{3+} ($S=1/2$), Ru^{5+} ($S=3/2$), and Mn^{3+} ($S=2$).

Our zero-field-cooled (ZFC) data for the magnetic moment $m_{\|}(T)$ along the easy **c** axis (Fig. 2) reveal a spontaneous magnetization that reflects FM correlations below $T_C=183$ K, consistent with previous polycrystalline data.[10] FC data for the magnetic moment $m_{\|}(T)$ did not exhibit any additional features, and retained the shape of the ZFC data, which indicates the behavior expected for conventional ferromagnets. The magnetization curves for $\boldsymbol{H}\|\mathbf{c}$ are characteristic of a soft FM material with a coercive field $H_{C\|}=400$ Oe at $T=5$ K (Fig. 2 inset). Distinct magnetic anisotropy (Figs. 2–4) indicates the **c** axis is the easy direction.

Striking behavior emerges for $\boldsymbol{H}\perp\mathbf{c}$ for which the ZFC moment exhibits *three distinct anomalies*: an abrupt increase just below $T_1=183$ K, followed by a cusp at $T_2=171$ K, and a sharp minimum at $T_3=128$ K that marks a strong linear increase of $m_{\perp}(T,H)$ with decreasing $T<\mathrm{T}_3$, as shown in Fig. 3. The sharp decrease of $m_{\perp}(T,H)$ below $T_2=171$ K

TABLE II. Atomic coordinates ($\times10^4$) and equivalent isotropic displacement parameters ($Å^2\times10^3$) for $BaMn_{2.49}Ru_{3.51}O_{11}$. U(eq) is defined as one-third of the trace of the orthogonalized Uij tensor.

	x	y	z	U(eq)
Ba(1)	3333	6667	2500	6(1)
Ru(1)	0	0	1497(1)	4(1)
Ru(2)	5000	0	0	10(1)
Mn(1)	0	0	1497(1)	4(1)
Mn(2)	5000	0	0	10(1)
Mn(3)	3333	6667	7500	14(1)
O(1)	1711(3)	3422(5)	800(2)	7(1)
O(2)	8544(4)	17087(8)	2500	7(1)
O(3)	3333	6667	5796(4)	17(1)

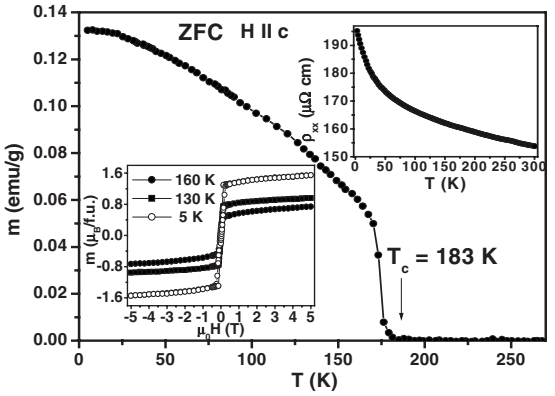

FIG. 2. ZFC magnetic moment $m_{\|}(T)$ vs temperature T of single-crystal $BaMn_{2.49}Ru_{3.51}O_{11}$. The arrow designates the magnetic ordering temperature T_C. The lower inset shows $m_{\|}(T,H)$ vs applied field $\mu_o \boldsymbol{H} \| \mathbf{c}$ for several temperatures. The upper inset shows ρ_{xx} vs temperature.

indicates AFM interactions, whereas the linear increase of $m_{\perp}(T,H)$ below $T_3=128$ K reflects residual FM correlations. In the present case of $BaMn_{2.49}Ru_{3.51}O_{11}$, frustrated AFM Mn-Mn interactions within the kagome lattice are supplemented by Mn-Ru and Ru-Ru interactions, which may explain the residual FM behavior observed for $\boldsymbol{H} \perp \mathbf{c}$. The inset in Fig. 3 shows $\chi_{\perp}(T,H) \equiv m_{\perp}/H$ in fields $(0.01 \leq \mu_o H \leq 1$ T) that slowly broaden and shift the T_2 anomaly to lower temperatures. We note that the sharp change in slope of the ZFC moment at $T_3=128$ K rapidly becomes indistinct for $\mu_o H > 0.05$ T, consistent with the dominance of residual FM correlations at low temperatures. All the above observations indicate a complex magnetic state.

In-plane magnetic interactions are reflected in the field dependence of $m_{\perp}(T,H)$ shown in Fig. 4. Two distinct regions are apparent just below 167 K: a slow, linear increase that ends at a critical field $H^*(T)$ at which $dm_{\perp}/dH$ is discontinuous, followed by a saturated regime above $H^*(T)$,

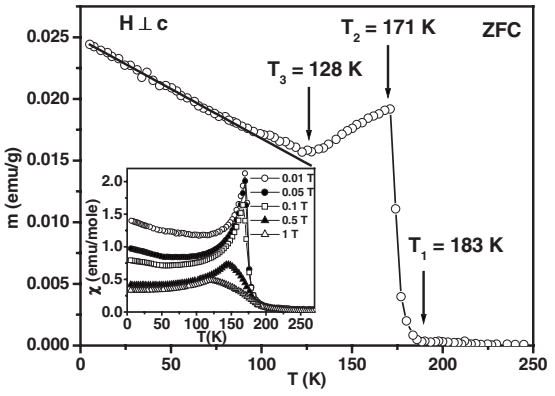

FIG. 3. Temperature dependence of the ZFC magnetic moment $m_{\perp}(T,H)$ of single-crystal $BaMn_{2.49}Ru_{3.51}O_{11}$. Arrows designate magnetic transition temperatures. The solid line illustrates the near-linear dependence below $T_3=128$ K. The inset shows $\chi_{\perp}(T,H) \equiv m_{\perp}/H$ at different applied fields $\mu_o \boldsymbol{H} \perp \mathbf{c}$. Note the rapid suppression of the anomalous linear behavior in applied fields of order 0.1 T.

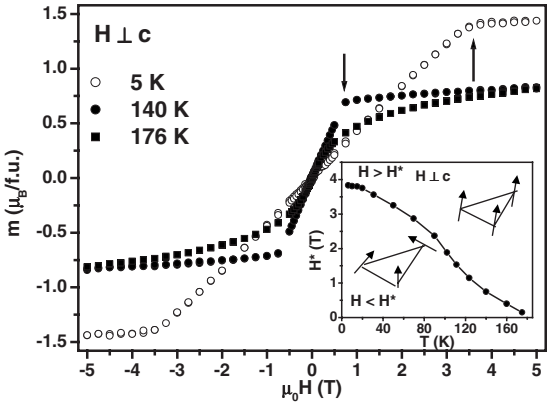

FIG. 4. Magnetic moment $m_{\perp}$ vs applied field $\boldsymbol{H} \perp \mathbf{c}$ for several temperatures T for single-crystal $BaMn_{2.49}Ru_{3.51}O_{11}$. The inset shows the inferred change of spin configuration traversing the critical field $H^*(T)$ (denoted by solid dots) indicated by arrows in the main panel.

whose magnitude increases with decreasing T. This behavior is comparable to simple AFM materials, where $m(H)$ barely changes in the low-field collinear phase, then abruptly jumps at a spin-flop transition to a canted structure exhibiting a strong linear increase of $m(H)$ that ends abruptly at FM saturation. The strong linear increase and *absence of any jump* in $m_{\perp}(H)$ in Fig. 4 suggests a canted spin arrangement (dominated by AFM correlations) is present below $T_2=171$ K. The linear portion of $m_{\perp}(H)$ is replaced by a nonlinear FM behavior above 171 K, which confirms AFM correlations yield to FM correlations for $T > T_2$.

Although complex, the magnetization behavior of $BaMn_{2.49}Ru_{3.51}O_{11}$ can be explained in terms of magnetic frustration, which can generate a nontrivial spin texture on the kagome sublattice. This scenario is corroborated by our deduction of a THE (Refs. 1 and 2) from our transverse magnetoresistivity $\rho_{xy}(H,T)$ data, as discussed below.

The Hall resistivity of ferromagnets is usually expressed as

$$\rho_{xy} = R_o H + 4\pi M R_s, \tag{1}$$

where R_o is the normal Hall coefficient resulting from the Lorentz force, and R_s is the anomalous Hall coefficient that is dependent upon the magnetization M and spin-orbit coupling.[13,14] The low-field Hall effect of FM materials is dominated by the anomalous Hall effect (AHE) that has roughly the same field dependence as $M(T,H)$ below T_C.[13]

We measured $\rho_{xy}(H,T)$ in single-crystal $BaMn_{2.49}Ru_{3.51}O_{11}$ with a standard, in-plane current $\boldsymbol{J} \perp \boldsymbol{H} \| \mathbf{c}$ (easy direction) configuration that we argue generates a large collinear magnetization that suppresses the scalar spin chirality and masks any THE. As expected, ρ_{xy} exhibits a nonlinear field dependence only for $H \ll 1.0$ T where the AHE dominates (upper inset, Fig. 5). Above 1.0 T, $m_{\|}(H)$ saturates (lower inset, Fig. 2) and ρ_{xy} exhibits a normal linear behavior with $d\rho_{xy}/dH = R_o = 1/nec$ (e is the electron charge, c is the speed of light and n is the carrier concentration), which yields $n \approx 10^{20}$ cm^{-3} and mobility $\mu = R_o/\rho \approx 3.5 \times 10^{-2}$ m^2 V^{-1} s^{-1} at $T=5$ K. The negative $d\rho_{xy}/dH$ is con-

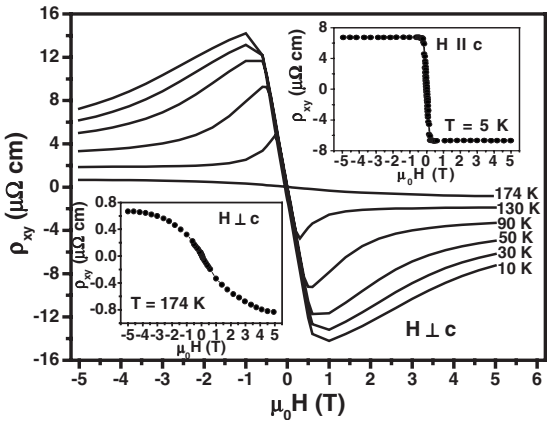

FIG. 5. Transverse resistivity ρ_{xy} versus magnetic field $\boldsymbol{H}\perp\mathbf{c}$ for single-crystal $BaMn_{2.49}Ru_{3.51}O_{11}$ at different temperatures. The upper inset shows ρ_{xy} versus magnetic field $\boldsymbol{H}\|\mathbf{c}$ (easy axis) at temperature $T=5$ K. The lower inset shows ρ_{xy} for a $BaMn_{2.49}Ru_{3.51}O_{11}$ single crystal at $T=174$ K and $\boldsymbol{H}\perp\mathbf{c}$.

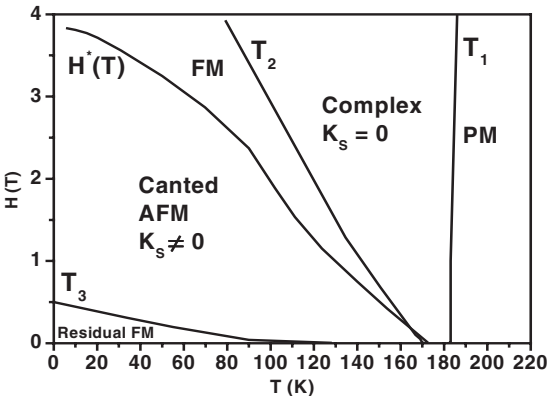

FIG. 6. A proposed magnetic-field-versus-temperature phase diagram of single-crystal $BaMn_{2.49}Ru_{3.51}O_{11}$ based upon magnetic and Hall-effect measurements with field $\mu_o\boldsymbol{H}\perp\mathbf{c}$. Symbol key: PM (paramagnetic), Complex $K_S=0$ (complex order, zero scalar chirality), AFM $K_S\neq 0$ (antiferromagnetic correlations, nonzero scalar chirality), FM (collinear ferromagnet, zero scalar chirality), and residual FM (unsaturated ferromagnetic order).

sistent with the weak low-T increase (for $T\leq 183$ K, ρ_{xx} is not thermally activated) and low value (153 $\mu\Omega$-cm at 300 K) of $\rho_{xx}(T,H=0)$ (upper inset, Fig. 2), which suggest $BaMn_{2.49}Ru_{3.51}O_{11}$ is a disordered metal.

The absence of magnetic anomalies in ρ near T_1, T_2, and T_3 is surprising and warrants discussion. Critical magnetic fluctuations depend upon the electronic mean-free path; as long as the mean-free path is smaller than a characteristic magnetic lattice spacing, critical magnetic fluctuations should not be prominent in electronic transport data. Indeed, the high resistivity of our samples is consistent with suppressed magnetic critical scattering. We also note that resistivity anomalies near magnetic ordering temperatures are absent in other high-resistivity transition-metal oxides such as single-crystal Sr_2IrO_4.[15]

To minimize the normal Hall term due to the Lorentz force induced by the external magnetic field, we applied $\boldsymbol{J}\|\boldsymbol{H}\perp\mathbf{c}$ and measured $\rho_{xy}(T,H)$ at various T, as shown in Fig. 5. In this unconventional configuration the transverse motion of carriers depends only on the AHE of the **c**-axis magnetization on the $M(2)$ and $M(3)$ sites, and the THE contribution of the nonzero scalar chirality of the $M(2)$ sublattice (here, we ignore the weak dipolar induction $\boldsymbol{B}\|\mathbf{c}$ exerted by ordered moments on the $M(2)$ and $M(3)$ sites[16]). In this geometry, $\rho_{xy}(T,H)$ for $\boldsymbol{T}<\boldsymbol{T}_2=171$ $\boldsymbol{K}$ exhibits high- and low-field regimes of behavior that correspond to the saturation behavior of $m(H)$ (see Fig. 5): $\rho_{xy}(H)$ exhibits a nearly linear decrease with increasing field for $|H|<\mathrm{H}^*$, followed by a sharp change in slope $d\rho_{xy}(H)/dH$. The field dependence of ρ_{xy} can be explained in terms of field suppression of the spin chirality. At low fields the tilting angle of spins is relatively large, which induces a large contribution to AHE; with further increases of field, spins increasingly align collinearly along the field direction and the spin chirality is reduced, which results in decreasing ρ_{xy}. $BaMn_{2.49}Ru_{3.51}O_{11}$ is unusual in that the peak in the ρ_{xy} approximately *triples in magnitude* between $T=130$ and 10 K in *fields well below* 1 T (Fig. 5). Note that for $T>171$ K, ρ_{xy} displays a monotonic field dependence typical for ferromagnets, implying there is *no THE or scalar chirality for* $\boldsymbol{T}_2<\boldsymbol{T}<\boldsymbol{T}_1$.

Our data for $BaMn_{2.49}Ru_{3.51}O_{11}$ can be understood by assuming frustrated AFM interactions lead to essentially two-dimensional spin correlations for $171<T<183$ K, which favors an in-plane, $q=0$ structure with uniform vector chirality on the kagome sublattice, as suggested by neutron-diffraction data[10] for polycrystalline $BaMn_2Ru_4O_{11}$, and our in-plane measurements of ρ_{xy} for single-crystal $BaMn_{2.49}Ru_{3.51}O_{11}$.[22] Below $T_2=171$ K, a **c**-axis moment starts to grow, caused by Dzyaloshinsky-Moriya interactions[17,18] appropriate for spins in the noncentrosymmetric structure of $BaMn_{2.49}Ru_{3.51}O_{11}$. The slow or incomplete saturation of the magnetization $m(T,H)$ with decreasing T, or increasing $\boldsymbol{H}\perp\mathbf{c}$, indicates an evolution from canted moments with AFM correlations within the kagome plane to a collinear FM arrangement. The spin canting out of the kagome plane induces nonzero scalar chirality $K_S=\boldsymbol{S}_1\bullet(\boldsymbol{S}_2\times\boldsymbol{S}_3)$ among spins $\boldsymbol{S}_i$ that occupy each of the three vertices of triangular plaquettes in the kagome plane (Fig. 4). The ρ_{xy} for $\boldsymbol{H}\perp\mathbf{c}$ is expected to scale with increasing $K_S\neq 0$ for $H<H^*(T)$ [the field at which $m(H)$ abruptly saturates]; but for $H>H^*(T)$, the spins reorient (inset of Fig. 4), causing K_S and ρ_{xy} to rapidly decrease with increasing field until the in-plane moment components completely align, leading to a collinear structure with $K_S=0$. Figure 6 depicts the magnetic phase diagram of $BaMn_{2.49}Ru_{3.51}O_{11}$, as inferred from magnetic and transport measurements for $\boldsymbol{H}\perp\mathbf{c}$.

In summary, we have observed three anomalies in low-field magnetization of a $BaMn_{2.49}Ru_{3.51}O_{11}$ single crystal at $T=128$, 171, and 183 K. The anomalies at 128 and 171 K are observed only for $\boldsymbol{H}\perp\mathbf{c}$. Our result $2(T_1-T_2)/(T_1+T_2)=(183\text{ K}-171\text{ K})/177\text{ K}=0.07$, recalls numerical studies of *XY* or planar triangular lattice systems[19] that predict spin and chiral order set in at two separate, but closely spaced temperatures that differ by no more than 8%.[20] Two distinct mechanisms for the Hall effect of $BaMn_{2.49}Ru_{3.51}O_{11}$ account

for our observations: An unusually strong, highly anisotropic, transverse magnetoresistivity is observed for magnetic field applied parallel to the kagome plane, as a consequence of a THE driven by nonzero scalar spin chirality. A smaller transverse magnetoresistivity, typical of AHE of FM materials with spin-orbit coupling, is observed for field applied perpendicular to the kagome plane.

$BaMn_{2.49}Ru_{3.51}O_{11}$ presents a unique example of a large THE in a magnetically ordered state.[21] The THE can be controlled by unusually modest applied fields $\mu_o H < 1$ T, implying low-field alteration of scalar spin chirality may provide a new way to control electronic properties in magnetic materials having requisite noncentrosymmetric structure. Clarification of the exact nature of the magnetic transitions below 183 K in $BaMn_{2.49}Ru_{3.51}O_{11}$ requires further theoretical work and neutron-scattering experiments on single crystals.

Research at the University of Kentucky was supported by U.S. DoE Grant No. DOE-FG∅2-97ER45653.

*Corresponding author; lshlyk@gmail.com

[1] Y. Taguchi, Y. Oohara, H. Yoshizawa, N. Nagaosa, and Y. Tokura, Science **291**, 2573 (2001).
[2] K. Ohgushi, S. Murakami, and N. Nagaosa, Phys. Rev. B **62**, R6065 (2000).
[3] T. Kimura, Ann. Rev. Mater. Res. **37**, 387 (2007).
[4] C. L. Henley, Phys. Rev. Lett. **62**, 2056 (1989).
[5] A. Kuroda and S. Miyashita, J. Phys. Soc. Jpn. **64**, 4509 (1995).
[6] A. B. Harris, C. Kallin, and A. J. Berlinsky, Phys. Rev. B **45**, 2899 (1992).
[7] A. Keren, Y. J. Uemura, G. Luke, P. Mendels, M. Mekata, and T. Asano, Phys. Rev. Lett. **84**, 3450 (2000).
[8] A. Keren, K. Kojima, L. P. Le, G. M. Luke, W. D. Wu, Y. J. Uemura, M. Takano, H. Dabkowska, and M. J. P. Gingras, Phys. Rev. B **53**, 6451 (1996).
[9] M. C. Cadee and D. J. W. Ijdo, J. Solid State Chem. **52**, 302 (1984).
[10] M. L. Foo, Q. Huang, J. W. Lynn, Wei-Li Lee, T. Klimczuk, I. S. Hagemann, N. P. Ong, and R. J. Cava, J. Solid State Chem. **179**, 563 (2006).
[11] B. Schüpp-Niewa, L. Shlyk, S. Kryukov, L. E. De Long, and R. Niewa, Z. Naturforsch. B **62**, 753 (2007).
[12] L. Shlyk, S. Kryukov, B. Schüpp-Niewa, R. Niewa, and L. E. De Long, Adv. Mater. **20**, 1315 (2008).
[13] R. Karplus and J. M. Luttinger, Phys. Rev. **95**, 1154 (1954).
[14] L. Berger, Phys. Rev. B **2**, 4559 (1970).
[15] S. Chikara, O. Korneta, W. P. Crummett, L. E. De Long, P. Schlottmann and G. Cao, Phys. Rev. B **80**, 140407(R) (2009).
[16] J. Ye, Y. B. Kim, A. J. Millis, B. I. Shraiman, P. Majumdar, and Z. Tesanovic, Phys. Rev. Lett. **83**, 3737 (1999).
[17] I. Dzyaloshinsky, J. Phys. Chem. Solids **4**, 241 (1958).
[18] T. Moriya, Phys. Rev. **120**, 91 (1960).
[19] H. Kawamura, arXiv:cond-mat/0202109 (unpublished).
[20] H. Kawamura, Phys. Rev. Lett. **82**, 964 (1999).
[21] D. Grohol, K. Matan, J.-H. Cho, S.-H. Lee, J. W. Lynn, D. G. Nocera, and Y. S. Lee, Nature Mater. **4**, 323 (2005).
[22] An empirical rule for the dependence of T_c on $3d/4d$ ratio for the ferrite family (Ref. 12) permits us to assume that the precise composition and magnetic structure of a previously studied powder [nominal composition $BaMn_2Ru_4O_{11}$ and $T_c = 185$ K (Ref. 10)] are very similar to that of our single-crystal ($T_c = 183$ K).